Verena C. Schulze Greiving*
Hans L. de Boer
Johan G. Bomer
Albert van den Berg
Séverine Le Gac**

BIOS, Lab on a chip Group, MESA+ Institute for Nanotechnology, MIRA Institute for Biomedical Technology and Technical Medicine, University of Twente, Enschede, The Netherlands

Received September 1, 2017
Revised November 4, 2017
Accepted November 5, 2017

Research Article

Integrated microfluidic biosensing platform for simultaneous confocal microscopy and electrophysiological measurements on bilayer lipid membranes and ion channels

Combining high-resolution imaging and electrophysiological recordings is key for various types of experimentation on lipid bilayers and ion channels. Here, we propose an integrated biosensing platform consisting of a microfluidic cartridge and a dedicated chip-holder to conduct such dual measurements on suspended lipid bilayers, in a user-friendly manner. To illustrate the potential of the integrated platform, we characterize lipid bilayers in terms of thickness and fluidity while simultaneously monitoring single ion channel currents. For that purpose, POPC lipid bilayers are supplemented with a fluorescently-tagged phospholipid (NBD-PE, 1% mol) for Fluorescence Recovery After Photobleaching (FRAP) measurements and a model ion channel (gramicidin, 1 nM). These combined measurements reveal that NBD-PE has no effect on the lipid bilayer thickness while gramicidin induces thinning of the membrane. Furthermore, the presence of gramicidin does not alter the lipid bilayer fluidity. Surprisingly, in lipid bilayers supplemented with both probes, a reduction in gramicidin open probability and lifetime is observed compared to lipid bilayers with gramicidin only, suggesting an influence of NBD-PE on the gramicidin ion function. Altogether, our proposed microfluidic biosensing platform in combination with the herein presented multi-parametric measurement scheme paves the way to explore the interdependent relationship between lipid bilayer properties and ion channel function.

Keywords:
Bilayer lipid membrane / Confocal microscopy / Gramicidin / Microfluidics / Single ion channel recordings
DOI 10.1002/elps.201700346

Additional supporting information may be found in the online version of this article at the publisher's web-site

1 Introduction

Understanding interactions between ion channels and their lipid surrounding is pivotal for fundamental research and drug development [1–3]. On one hand, conformational changes accompanying ion channel function can locally alter the lipid bilayer characteristics [4]. On the other hand, the lipid bilayer properties can modulate ion channel function through direct or indirect mechanisms [3,5]. For instance, different values have been recorded for the activation voltage of the voltage-dependent K+ channel (Kv) "paddle chimera" for oocyte-like and POPE:POPG lipid bilayers [6]. Similarly, the activation of MscL, an *Escherichia coli* mechanosensitive ion channel, varies as a function of the lipid bilayer thickness [7].

Ion channel function is typically characterized using electrophysiological measurements [8]. This approach provides a wealth of high-content information on single channel behavior such as insights into the conductance and possible

Correspondence: Dr. Séverine Le Gac, Applied Microfluidics for BioEngineering Research, MESA+ Institute for Nanotechnology, MIRA Institute for Biomedical Technology and Technical Medicine, University of Twente, Enschede, The Netherlands
E-mail: legac@utwente.nl

Abbreviations: BLM, bilayer lipid membrane; **DMPC**, 1,2-Dimyristoyl-sn-glycero-3-phosphorylcholine; **FRAP**, fluorescence recovery after photobleaching; **NBD**, N-(7-nitro-2-1, 3-benzoxadiazol-4-yl; **PE**, 1,2-dioleoyl-sn-glycero-3-phosphoethanolamine; **POPC**, 1-palmitoyl-2-oleoyl-sn-glycero-3-phosphocholine; **POPE**, 1-palmitoyl-2-oleoyl-sn-glycero-3- phosphoethanolamine; **POPG**, 1-palmitoyl-2-oleoyl-sn-glycero -3-phospho-(1'-rac-glycerol); **ROI**, region of interest

*Current address: Science, Technology and Policy Studies (STePS), MESA+ Institute for Nanotechnology, University of Twente, The Netherlands
**Current address: Applied Microfluidics for BioEngineering Research, MESA+ Institute for Nanotechnology, MIRA Institute for Biomedical Technology and Technical Medicine, University of Twente, Enschede, The Netherlands

Colour Online: See the article online to view Figs. 1–4 in colour.

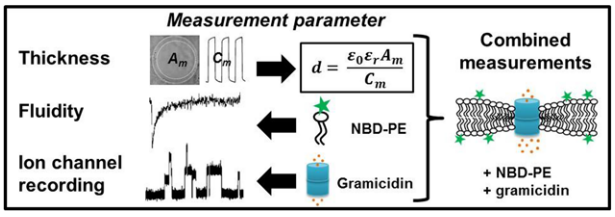

Figure 1. Multi-parametric characterization of lipid bilayers and simultaneous single ion channel recording. The thickness of the lipid bilayer is derived from its surface area (*Am*) and capacitance (*Cm*). Fluorescently-tagged phospholipids (1% NBD-PE) are added to the lipid bilayer to assess its fluidity through FRAP measurements and the determination of NBD-PE diffusion coefficient (*D*). Simultaneously, gramicidin single ion channel currents are recorded, after addition of gramicidin to the lipid bilayer (1 nM). This comprehensive approach allows correlating the lipid bilayer properties and single ion channel function.

sub-conductance states of individual pores, ion channel gating mechanism, ion channel open probability and kinetics [9], with a sub-picoampere and sub-millisecond resolution. However, electrophysiological recordings are blind to the nature of the ions transported through the pore, unless the buffer includes only specific ions [9]. Additionally, in this scenario, the lipid bilayer properties, which can influence ion channel function [10], are only assessed globally in terms of seal resistance and capacitance, and local changes in the lipid bilayer are not accessible. To obtain this missing information and to understand the interdependence of ion channel behavior and lipid bilayer properties, complementary strategies are required that couple electrophysiology with orthogonal measurement techniques. In that context, high-resolution microscopy is highly attractive, since it allows evaluating the lipid bilayer fluidity [11], phospholipid phase separation [12], the position and mobility of ion channels in the lipid matrix [13, 14] and the ion flux through individual ion channels [15, 16]. For simultaneous high-resolution imaging and electrophysiological measurements, a microfluidic format is particularly interesting, due to the horizontal configuration of the lipid bilayer.

Gramicidin, a linear peptide produced by the bacterium *Bacillus brevis* [17], is a well-established model for ion channels [18]. Gramicidin pore formation occurs upon dimerization of two non-conducting monomers present in each leaflet of the lipid bilayer [19], which involves local deformation of the lipid bilayer (compression and bending). Since the associated energetic cost for this deformation depends on the lipid bilayer properties (*i.e.*, fluidity, thickness, bending and compression modulus, intrinsic monolayer curvature, and stiffness) [20], gramicidin is ideally suited to study the relationship between lipid bilayer properties and ion channel function [17, 20–22] and it acts as a molecular force sensor in a lipid bilayer [20, 23].

In previous work, we developed a microfluidic device for experimentation on lipid bilayers, which is compatible with both electrophysiological and (high-resolution) microscopy measurements. These modalities have however been implemented in a separate way so far for, respectively, recording single ion channel currents and imaging phospholipid phase separation [24]. Here, we report simultaneous confocal microscopy measurements and electrophysiological recordings on single ion channels inserted in a suspended lipid bilayer in our microfluidic platform. First, an integrated biosensing platform is developed to perform these comprehensive measurements. Next, the impact of the lipid bilayer properties on gramicidin ion channel function is studied. Specifically, the lipid bilayer thickness (derived from the specific capacitance) and fluidity (evaluated through FRAP measurements) are simultaneously determined, while recording gramicidin single ion channel currents (See Fig. 1).

2 Materials and methods

2.1 Materials

Membranes are prepared from POPC (1-palmitoyl-2-oleoyl-sn-glycero-3-phosphocholine) and NBD-PE (1,2-dioleoyl-sn-glycero-3-phosphoethanolamine-N-(7-nitro-2-1,3-benzoxadiazol-4-yl) (ammonium salt)), both purchased as solutions in chloroform from Avanti Polar lipids (Alabaster, AL, USA). Potassium chloride (KCl), (4-(2-hydroxyethyl)-1-piperazineethanesulfonic acid (Hepes) and gramicidin (mixture of species with ~80% gramicidin A) are obtained from Sigma Aldrich (Zwijndrecht, The Netherlands), n-decane from Fluka (Steinheim, Germany), and ethanol from Assink Chemie (Enschede, The Netherlands). Deionized water (MilliQ system, Millipore, Billerica, MA, USA) is used for the preparation of all aqueous solutions.

2.2 Microfluidic device

The core of the integrated biosensing platform is a microfluidic device [24, 25], which consists of two borofloat glass substrates separated by a 12.5-μm thin Teflon foil (Sabic BV Snij-Unie HiFi, Enkhuizen, The Netherlands). Each glass substrate comprises one microfluidic channel (100 μm deep, 300 μm wide) and the Teflon foil an aperture (100 μm diameter), which is located at the channel intersection. For confocal microscopy imaging, the bottom glass substrate is thinned down from 500 μm to ~200 μm by manual polishing (Vanhespen optics, Borne, The Netherlands). The bonding procedure is slightly adapted due to the fragility of the thinned bottom substrate: the Teflon foil is first bonded to the top glass substrate using UV-curable adhesive (NOA81, Norland Optical Adhesives), followed by the bottom substrate.

2.3 Fabrication of the integrated biosensing platform and packaging

For simultaneous confocal and electrophysiological measurement, the microfluidic device is placed in a dedicated

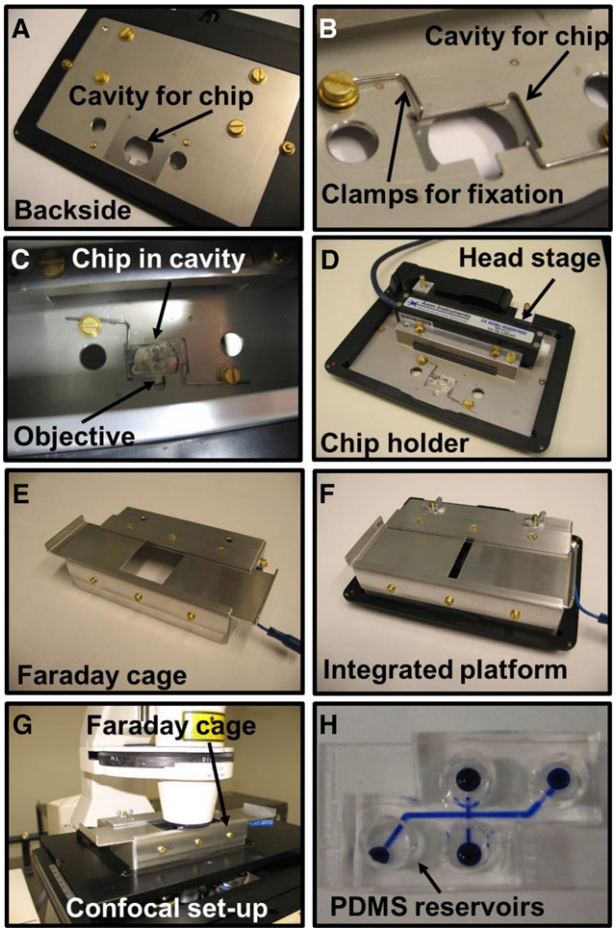

Figure 2. Integrated biosensing platform for simultaneous electrophysiological and confocal microscopy measurements. A dedicated chip-holder is integrated in a microscope plate; it includes a cavity (A) to house the microdevice which is secured with clamps (B), and to allow contact with the oil-immersion objective (C). For electrophysiological measurements, the head stage of the patch-amplifier (D) is integrated in the platform. A miniaturized Faraday cage (E and F) closes the chip-holder. This Faraday cage includes sliding parts to access the microfluidic device. The platform fits on the stage of the confocal microscope (G). Finally, a PDMS layer with large openings (3.4 mm diam.) acting as fluid reservoirs, is bonded on the device (H).

chip-holder, which fits on the stage of an inverted confocal microscope (Fig. 2). Specifically, a stainless steel plate with a hole for the microfluidic device is cut with a laser to fit in the frame of the microscope (Zeiss mounting frame K-X, anodized aluminum, Sliedrecht, The Netherlands) and manually finished with a file. A smaller stainless steel plate is similarly realized, and connected from the back of the inlay to the hole by spot welding to form a matching cavity for the microfluidic device (Fig. 2A and B). The cavity is equipped with two spring steel clamps, held in place by brass screws, to secure the device (Fig. 2B and C). An aluminum bar is screwed to the bottom plate of the holder to secure the CV 203 BU head stage of the Axopatch 200B amplifier (Molecular Devices, Sunnyvale, CA, USA) (Fig. 2D). For electrophysiological measurements, the head stage and Ag/AgCl electrodes (Molecular devices) are shielded by an aluminum Faraday cage having sliding parts to access to the microfluidic device during the experiments (Fig. 2E–G). A brass screw connects the microscope frame with the inlay plate and the Faraday cage to ensure proper grounding. Reservoirs (~3.4 mm diameter) are punched in a thick slab (~4.4 mm thickness) of PDMS (Sylgard 184, Dow Corning, Farnell, Maarssen, The Netherlands, Fig. 2H), which is subsequently bonded to the microfluidic device after plasma activation (Harrick Scientific Products, NY, USA).

2.4 Bilayer lipid membrane experimentation and characterization

Bilayer lipid membranes are formed as described previously [24] by introducing 0.5 μL lipid solution (25 mg/mL in n-decane) in both channels, followed by 30 and 20 μL of buffer solution (1 M KCl, 10 mM Hepes, pH 7.4) in the bottom and top channel, respectively. The seal resistance R_m is assessed by applying a dc voltage (10 mV, ~5 s) while recording the current response, and derived from $R_m = V_{applied} / (I_{applied\ voltage} - I_{voltage=0})$. The surface area is measured from a wide-field picture (ImageJ open source software from NIH). The capacitance is determined as detailed in supplementary material (see S1). All capacitance values are corrected for the stray capacitance (0.84 ± 0.27 pF, $n = 2$) measured in a device filled with lipid solution.

2.5 Simultaneous confocal and electrophysiological measurements

FRAP measurements are conducted with a laser scanning confocal microscope (LSM510 Zeiss, Argon laser, $\lambda =$ 488 nm, plan-apochromat 63x/1.4 oil DIC objective, LP 505 filter and HFT 488 beam splitter). Two regions of interest (ROIs) (15-μm diameter), a measurement region and a reference region, are defined in the center of the lipid bilayer with 10-μm spacing. The z position is adjusted for the maximal fluorescence intensity. The measurement ROI is bleached by ~22% followed by recovery, and this procedure is repeated at least twice per lipid bilayer. The background fluorescence is determined after rupture of the lipid bilayer by applying a high voltage pulse (~1.3 V, 'zapping'). Data are processed using FRAPAnalyser (freeware from the University of Luxemburg, http://actinsim.uni.lu/eng) to derive the diffusion coefficient (D) of the fluorescently-tagged phospholipids NBD-PE. Simultaneously, gramicidin single ion channels are recorded. Specifically, a dc voltage of 80 mV is applied, and the current continuously recorded (1 kHz Low-pass Bessel filter, 10 kHz sampling rate). Data are filtered and analyzed using an in-house written Matlab routine to determine the open probability, number of channels, average single channel lifetime and single channel conductance. All experiments are carried

out at room temperature, but without any precise temperature control in the device.

3 Results

3.1 Integrated platform for simultaneous electrophysiological measurements and high-resolution imaging

The integrated platform has been designed for simultaneous electrophysiological measurements and high-resolution imaging (Fig. 2). A cavity is machined in the bottom plate of the microscope frame for allowing contact between the bottom substrate of the microfluidic device and the 63x oil-immersion objective, which is a premise for high-resolution imaging. Due to the small footprint of the microfluidic device (1 cm x 2 cm), a trade-off must be made between having enough space for the microdevice to contact the objective, on one hand, and creating enough support to hold the device, on the other hand. Here, a metal plate is welded to the backside of the hole in the microscope stage to provide support at the edges of the device while leaving a large opening in the center for the oil-immersion objective to approach the bottom substrate. In this configuration, the distance between the microscope objective and the lipid bilayer is *ca.* 200–210 μm depending on the exact thickness of the bottom glass substrate and the z-position of the lipid bilayer in the aperture (Supporting Information Fig. 2), which allows performing high-resolution imaging of the lipid bilayer. Figure 3 presents pictures of a free-standing lipid bilayer recorded by bright-field and confocal microscopy, as well as typical FRAP measurement curves.

The microfluidic device is covered with a thick PDMS slab including reservoirs, which are filled with 20–30 μL of buffer to prevent significant evaporation in the device during experimentation. Previously, in absence of reservoirs, liquid in the channels was evaporating quickly [24], which compromised the lipid bilayer stability and resulted in its bending, precluding thereby high resolution imaging (Supporting Information Fig. 3). In contrast, here, the lipid bilayers remained stable for up to 10 h, allowing recording ion channels under continuous application of an 80-mV voltage. No deterioration of the lipid bilayer characteristics (sealing resistance, surface area, and specific capacitance) was observed, as checked before and after experimentation (stability of the specific capacitance shown in Supporting Information Fig. 4). PDMS is also transparent, which allows bright-field microscopy imaging to determine the lipid bilayer surface area. Additionally, the PDMS reservoirs better secure the Ag/AgCl electrodes, which are inserted in the device inlets, compared to our previous chip-holder [24]. We have characterized the specifications of our set-up for electrophysiological recordings. Using a 1-kHz Low-pass Bessel filter allows minimizing the electrical noise (Supporting Information Fig. 5). Furthermore, the noise level during gramicidin ion channel recordings is as low as 0.3 pA (Fig. 3).

3.2 Correlating lipid bilayer properties and single ion channel function

Using this integrated biosensing platform, we propose a comprehensive measurement protocol depicted in Fig. 1, to simultaneously characterize lipid bilayer properties (thickness and fluidity) and record single ion channel function (Fig. 3). To

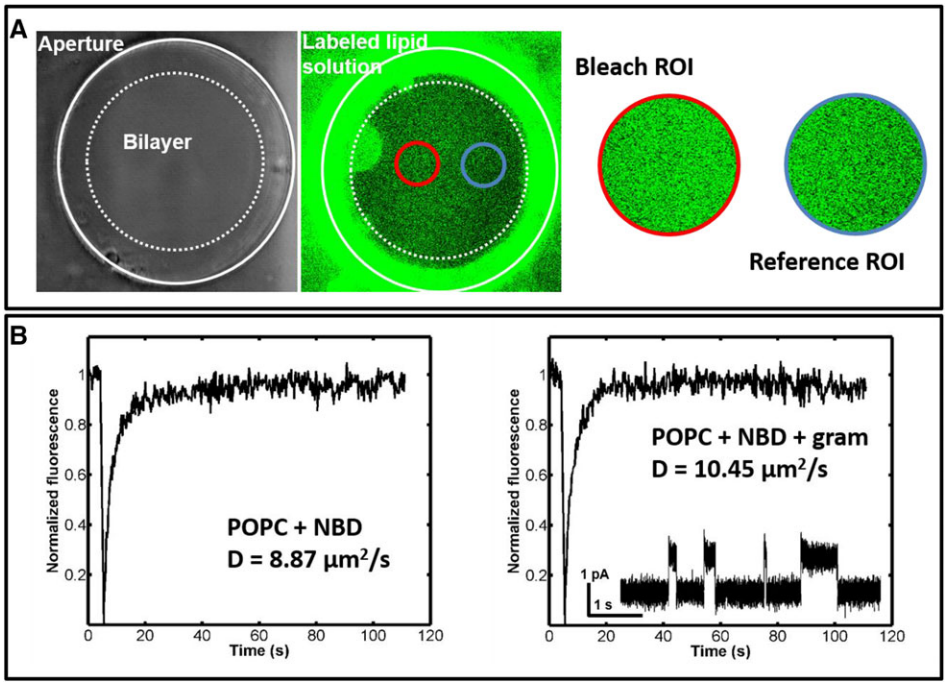

Figure 3. Simultaneous FRAP and electrophysiological measurements (A) Bright-field (left) and confocal fluorescence images (right) of a free-standing lipid bilayer in the microfluidic platform. For FRAP measurements, two bleach and reference ROIs are defined in the center of the lipid bilayer. (B) FRAP curves and corresponding diffusion coefficients for lipid bilayers without (left) and with (right) gramicidin. Inset: gramicidin electrophysiological recording simultaneous to the FRAP measurements.

that end, two probe molecules are added to the lipid bilayer: a fluorescently-tagged phospholipid NBD-PE (1% mol) to assess the lipid bilayer fluidity through FRAP measurements, and the ion channel gramicidin (1 nM, peptide/lipid molar ratio of $\sim 3 \times 10^{-8}$).

First, all lipid bilayers (with both probes, either probe and no probe) are characterized in terms of seal resistance (R_m), capacitance (C_m) and surface area (A_m), as summarized in Supporting Information Table 6. In a next step, the specific capacitance of the lipid bilayers ($C_s = C_m / A_m$) is derived, and their thickness assessed using $d = \varepsilon_0 \varepsilon_r / C_s$, where ε_0 is the permittivity of free space and ε_r the dielectric constant of the lipid bilayer. Here, a value of 2.09 for ε_r is used for all lipid bilayers. In general, the dielectric constant of hydrocarbons lies in the 2–4 range [26], and this specific value has previously been reported for PC lipid bilayers in n-decane [27]. Furthermore, no influence of the NBD group on the dielectric constant ε_r is anticipated, since this fluorophore is attached to PE head group. Finally, gramicidin has been reported not to significantly affect the lipid bilayer dielectric properties [28]. The specific capacitance values of NBD-PE containing lipid bilayers without and with gramicidin are 0.52 ± 0.10 and 0.57 ± 0.03 $\mu F/cm^2$ (both $n = 5$), which corresponds to thicknesses of 3.65 ± 0.64 and 3.28 ± 0.18 nm, respectively (Table 1). Overall, these specific capacitance and thickness values are similar to those of plain POPC bilayers (0.54 ± 0.02 $\mu F/cm^2$ and 3.45 ± 0.16 nm, both $n = 6$, Table 1). Interestingly, lipid bilayers containing only gramicidin exhibit a higher specific capacitance (0.65 ± 0.03 $\mu F/cm^2$, $n = 4$) and a decreased lipid bilayer thickness (2.86 ± 0.15 nm ($n = 4$)) (Table 1). A first possible explanation for the increase in C_s is that channels, which are open during the capacitance measurements, would lead to a distortion of the recorded current and an over-estimation of the capacitance. However, the capacitance values have been corrected for possible leakage currents to compensate for this potential effect (see Supporting Information 1). Therefore, another factor must play a role here. Upon gramicidin dimerization, the lipid bilayer must thin down locally to match the hydrophobic length of the gramicidin channel (2.17 nm) [29, 30]. In solvent-containing lipid bilayers, like here, this phenomenon is accompanied by solvent expulsion from the lipid bilayer, and subsequent compression of the phospholipid hydrocarbon chains in proximity to the channel [19, 31]. Subsequently, the lipid bilayer thickness in the direct vicinity of the gramicidin channel is comparable to that of solvent-free lipid bilayers [32]. Interestingly, according to recent reports, such changes induced by gramicidin in the lipid bilayer structure (*e.g.*, thickness and phospholipid organization) are not only local, but also more global [33], even at low gramicidin concentration in the lipid bilayer (1:10^5 gramicidin:lipid ratio) [34]. So, altogether, we hypothesize that gramicidin dimerization would result in the global decrease in the lipid bilayer thickness, we find here. It should however be noted that such thinning of the lipid bilayer is not found when both probe molecules are present, as discussed later in this article.

Next, the diffusion coefficient (D) of fluorescently-tagged phospholipids (NBD-PE) is evaluated, as a measure for the lipid bilayer fluidity (Fig. 4A, Table 1). For lipid bilayer with only NBD-PE, a value of 8.97 ± 0.90 $\mu m^2/s$ ($n = 5$) is found, which is similar to previously reported data for suspended PC lipid bilayers [11, 35]. Our D values are higher than those found for supported POPC bilayer lipid membranes at 25°C (4.2 ± 0.4 $\mu m^2/s$) [36], which can be explained by the fact that diffusion is decreased in presence of a solid substrate. The addition of gramicidin does not affect significantly the lipid bilayer fluidity ($D = 9.37 \pm 3.88$ $\mu m^2/s$ ($n = 5$)). Gramicidin has been reported to induce chain ordering in DMPC lipid bilayers, but at a much higher peptide/lipid ratio (7×10^{-2}) [37, 38] than here ($\sim 3 \times 10^{-8}$). Finally, variations are observed in the measured diffusion coefficient, which we attribute to thermal fluctuations, since all experiments are carried out at room temperature, but without any precise control on the temperature in the device.

Simultaneously, gramicidin single channels are recorded in POPC lipid bilayers without ($n = 4$) and with NBD-PE ($n = 5$) (Fig. 4B). Data are recorded for 1209 and 2327 s (total numbers of channels of 365 and 368), for lipid bilayers without and with NBD-PE, respectively. Single ion channel recordings are analyzed in terms of open probability, channel lifetime (τ) and single channel conductance (g). First, the open probability is determined by dividing the sum of the lifetimes of all channels by the total recorded time for each experiment (t_{open}/t_{total}), and open probabilities of 0.37 ± 0.06 and 0.13 ± 0.11 are respectively determined for lipid bilayers without and with NBD-PE (Fig. 4B and c *top*). Next, the

Table 1. Bilayer lipid membrane properties

POPC BLM	C_s ($\mu F/cm^2$)	d (nm)	D ($\mu m^2/s$)	t_{open}/t_{total}	τ (s)	g (pS)
No probe[a)]	0.54 ± 0.02	3.45 ± 0.16	-	-	-	-
+ NBD-PE[b)]	0.52 ± 0.10	3.65 ± 0.64	8.97 ± 0.90	-	-	-
+Gramicidin[c)]	0.65 ± 0.03	2.86 ± 0.15	-	0.37 ± 0.06	1.22	16.4
+ NBD-PE & gramicidin[b)]	0.57 ± 0.03	3.28 ± 0.18	9.37 ± 3.88	0.13 ± 0.11	0.74	16.7

Specific capacitance (C_s), bilayer lipid membrane thickness (d) and diffusion coefficient (D), as well as gramicidin open probability (t_{open}/t_{total}), average single channel lifetime (τ), and single channel conductance (g). Bilayer lipid membranes (BLM) formed from POPC (25 mg/mL) in n-decane, supplemented with 1% mol NBD-PE, 1 nM gramicidin, both probe molecules or no probe.

a) $n = 6$.

b) $n = 5$.

c) 4, ± SD.

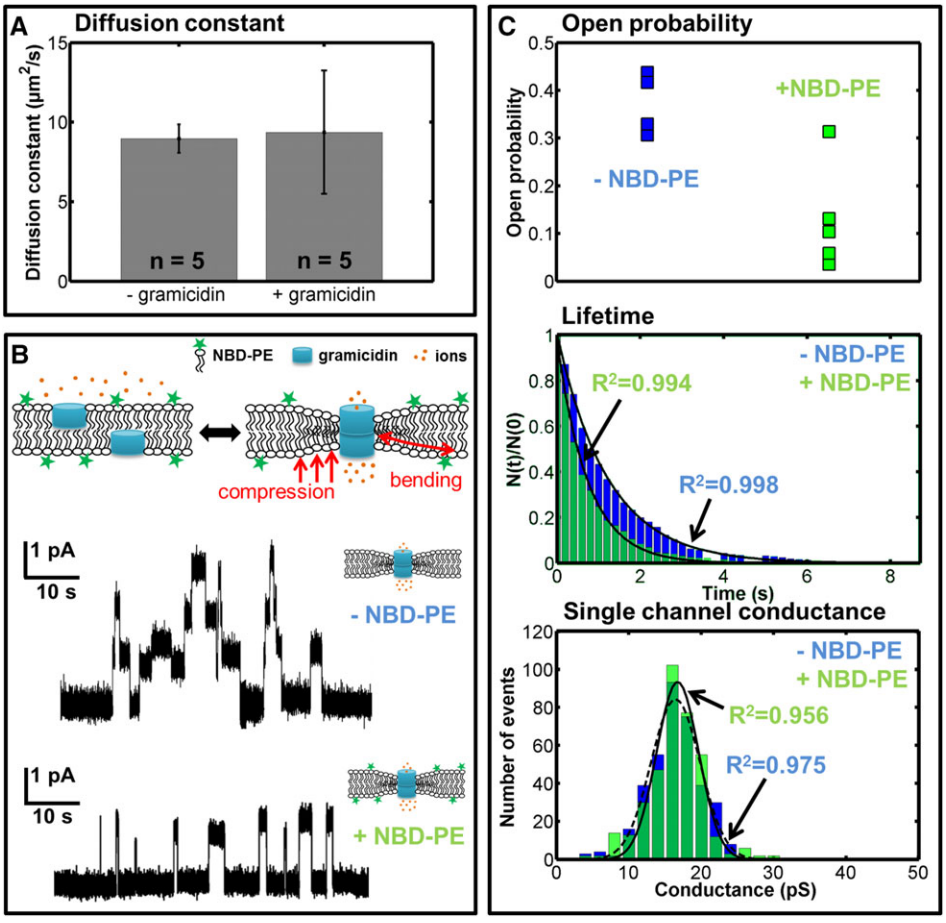

Figure 4. Gramicidin single ion channel recordings. (A) Diffusion coefficients (*D*) of NBD-PE determined using FRAP for lipid bilayers formed from POPC (25 mg/mL in n-decane), supplemented with 1% mol NBD-PE, without (green) and with (blue) 1 nM gramicidin. Error bars represent the standard deviation between different experiments ($n = 5$). (B) Schematic representation of the gramicidin pore formation process, NBD-PE being present in the lipid bilayer (top). Gramicidin single ion channel recordings in POPC lipid bilayers without (middle) and with (bottom) NBD-PE. (C) Analysis of gramicidin function in lipid bilayers without (blue) and with (green) NBD-PE: open probability (top), lifetime (middle), and single channel conductance (right). Bin size lifetime: 0.2 s, bin size conductance: 2 pS. Experimental conditions: 1 M KCl buffer, applied dc voltage of 80 mV, sampling rate of 10 kHz.

channel lifetime is plotted (Fig. 4C *middle*) [20, 39]. Specifically, the number of channels with various lifetimes is plotted as $N(t)$, which is defined as the total number of channels with a lifetime longer than t, and normalized with $N(0)$, the total number of recorded channels. This distribution is fitted using an exponential fit, and the average single channel lifetime τ is derived from $N(t)/N(0) = \exp(-t/\tau)$. Here, average single channel lifetime values of 1.22 and 0.74 s are found for lipid bilayers without and with NBD-PE, respectively. Last, the single channel conductance (g) is examined, and its distribution fitted with a Gaussian curve. Both series of experiments yield similar distributions (Fig. 4c *bottom*), with average conductance values of 16.4 pS and 16.7 pS for lipid bilayers without (dashed line) and with (solid line) NBD-PE, respectively, which is in good agreement with previous reports [24, 40]. The spread in the conductance is likely caused by the fact that we use a gramicidin mixture (with ~80% gramicidin A), which present different single channel conductance states [41]. All data are summarized in Table 1.

4 Discussion

Altogether, and surprisingly, these experiments reveal that the presence of NBD-PE has an impact on the gramicidin single channel function. As mentioned earlier, the gramicidin ion channel function can be influenced by various lipid bilayer properties (thickness, fluidity or mechanical properties) [18, 20, 42], as well as through specific peptide-lipid interactions [22]. Here, the lipid bilayer thickness is not altered in presence of NBD-PE alone (Table 1), and the possible influence of NBD-PE on the fluidity cannot easily be evaluated since FRAP measurements require its presence in the lipid bilayer. Furthermore, our platform does not allow accessing the lipid bilayer mechanical properties. PE has an inverted conical shape, which confers a negative curvature to the lipid bilayer [20], which in turn impacts gramicidin ion function [20, 42]. However, in contrast to PE, NBD-PE has a cylindrical shape due to the presence of the bulky NBD fluorophore, so that NBD-PE has no such effect on the lipid bilayer curvature [43]. Altogether, indirect mechanisms through an alteration of the lipid bilayer properties can very likely be excluded here. Therefore, we hypothesize that polar interactions take place between the hydrophobic and polar NBD moiety and indole groups on Trp residues at the C-term side of the gramicidin monomer. These peptide-lipid specific interactions would hinder the required conformational changes of both the gramicidin and its neighboring phospholipid(s) for gramicidin dimerization and formation of a conducting pore [44], and subsequently lead to a decrease in

gramicidin pore formation, as observed here (Table 1). Similarly, these interfacial polar interactions between the peptide and the lipid head group would lead to a reduction in the ion channel lifetime [22], as measured here (Table 1). Remarkably, this alteration in gramicidin function caused by the presence of NBD-PE clarifies the difference in thickness we observe for lipid bilayers supplemented with gramicidin only and gramicidin and NBD-PE (Table 1). Since thinning of gramicidin-containing lipid bilayers is accounted for by solvent expulsion upon gramicidin pore formation, a reduction in gramicidin open probability, as observed here in presence of NBD-PE, would prevent the lipid bilayer from thinning. Last, no significant variation is detected in the single channel conductance for the different sets of experiments. According to the literature, the gramicidin single ion channel conductance is not affected by the lipid bilayer properties but by the dipole moment of the lipids in the vicinity of the gramicidin pore [32, 39]. In our case, while the head groups of NBD-PE and PC have different properties (charge and dipole moment), we hypothesize that only PC phospholipids would be in the vicinity of a conducting ion channel, which would explain the similarity in the conductance we observe in our experiments.

4.1 Conclusion

Here, we have described an integrated biosensing platform consisting of a microfluidic device and a dedicated holder for simultaneous electrophysiological recordings and high-resolution imaging for user-friendly multi-parametric measurements on freestanding lipid bilayer models, including characterization of their thickness, fluidity and single ion channel recordings. The herein presented biosensing platform and associated comprehensive measurement approach open a new avenue for understanding the reciprocal influence of ion channels and lipid bilayer properties. In the future, it would be interesting to apply this multi-parametric measurement scheme to investigate biologically relevant ion channels known to be sensitive to their lipid environment such as sodium channels [45], or to link ion channel function to phospholipid phase separation and membrane dynamics. Finally, our platform would be of great value to identify non-specific effects of drugs on ion channel function via alterations in the lipid bilayer properties, an aspect which should not be neglected in the process of drug development [46].

The authors would like to thank Dr. Martin Bennink for lending the patch-amplifier, and Burcu Celikkol, Aditya Iyer, and Himanshu Chaudhary for their help with the FRAP measurements. This work is supported by NanoNextNL, a micro and nanotechnology consortium of the Government of the Netherlands and 130 partners. S. L. G. would like to thank financial support of the MESA+ Institute for Nanotechnology through the strategic research orientation "Nanotechnology for Innovative Medicine".

The authors have declared no conflict of interest.

5 References

[1] Ashcroft, F. M., *Nature* 2006, *440*, 440–447.

[2] Hille, B., *Ion Channels of Excitable Membranes*, Sunauer Associates Inc., Sunderland, MA, USA 2001.

[3] Lee, A. G., *Mol. BioSys.* 2005, *1*, 203–212.

[4] Phillips, R., Ursell, T., Wiggins, P., Sens, P., *Nature* 2009, *459*, 379–385.

[5] Lundbæk, J. A., Andersen, O. S., *Cholesterol Regulation of Ion Channels and Receptors*, John Wiley & Sons, Inc, Hoboken 2012, pp. 27–44.

[6] Schmidt, D., MacKinnon, R., *Proc. Nat. Ac. Sci. USA* 2008, *105*, 19276–19281.

[7] Perozo, E., Kloda, A., Cortes, D. M., Martinac, B., *Nat. Struct. Mol. Biol.* 2002, *9*, 696–703.

[8] Hamill, O. P., Marty, A., Neher, E., Sakmann, B., Sigworth, F. J., *Pflug. Arch. Eur. J. Phys.* 1981, *391*, 85–100.

[9] Aidley, D. J., Stanfield, P. R., *Ion Channels*, Cambridge University Press, Cambridge 1996.

[10] Tillman, T., Cascio, M., *Cell Biochem. Biophys.* 2003, *38*, 161–190.

[11] Ladha, S., Mackie, A. R., Harvey, L. J., Clark, D. C., Lea, E. J., Brullemans, M., Duclohier, H., *Biophys. J.* 1996, *71*, 1364–1373.

[12] Honigmann, A., Walter, C., Erdmann, F., Eggeling, C., Wagner, R., *Biophys. J.* 2010, *98*, 2886–2894.

[13] Veatch, W. R., Mathies, R., Eisenberg, M., Stryer, L., *J. Mol. Biol.*. 1975, *99*, 75–92.

[14] Ide, T., Yanagida, T., *Biochem. Biophys. Res. Co.* 1999, *265*, 595–599.

[15] Heron, A. J., Thompson, J. R., Cronin, B., Bayley, H., Wallace, M. I., *J. Am. Chem. Soc.* 2009, *131*, 1652–1653.

[16] Hemmler, R., Bose, G., Wagner, R., Peters, R., *Biophys. J.* 2005, *88*, 4000–4007.

[17] Kelkar, D. A., Chattopadhyay, A., *Biochom. Biophys. Acta (BBA) - Biomembranes* 2007, *1768*, 2011–2025.

[18] Lundbaek, J. A., Birn, P., Girshman, J., Hansen, A. J., Andersen, O. S., *Biochemistry* 1996, *35*, 3825–3830.

[19] Lundbaek, J. A., Andersen, O. S., *Biophys. J.* 1999, *76*, 889–895.

[20] Lundbaek, J. A., Collingwood, S. A., Ingolfsson, H. I., Kapoor, R., Andersen, O. S., *J.Roy. Soc. Interf.* 2010, *7*, 373–395.

[21] Andersen, O. S., Koeppe, R. E., *Ann. Rev. Biophys. Biomol. Struct.* 2007, *36*, 107–130.

[22] Rostovtseva, T. K., Petrache, H. I., Kazemi, N., Hassanzadeh, E., Bezrukov, S. M., *Biophys. J.* 2008, *94*, L23-L25.

[23] Ryu, H., Lee, H., Iwata, S., Choi, S., Kim, M. K., Kim, Y. R., Maruta, S., Kim, S. M., Jeon, T. J., *Sci. Rep.* 2015, *5*.

[24] Stimberg, V. C., Bomer, J. G., van Uitert, I., van den Berg, A., Le Gac, S., *Small* 2013, *9*, 1076–1085.

[25] Bomer, J. G., Prokofyev, A. V., van den Berg, A., Le Gac, S., *Lab Chip* 2014, *14*, 4461–4464.

[26] Heimburg, T., *Thermal Biophysics of Membranes*, Wiley-VCH Verlag GmbH & Co. KgaA, Weinheim 2007.

[27] Fettiplace, R., Andrews, D. M., Haydon, D. A., *J. Memb. Biol.* 1971, *5*, 277–296.

[28] Bransburg-Zabary, S., Kessel, A., Gutman, M., Ben-Tal, N., *Biochemistry* 2002, *41*, 6946–6954.

[29] Elliott, J. R., Needham, D., Dilger, J. P., Haydon, D. A., *Biochim. Biophys. Acta* 1983, *735*, 95–103.

[30] Killian, J. A., *Biochim. Biophys. Acta (BBA) - Biomem.* 1998, *1376*, 401–416.

[31] Helfrich, P., Jakobsson, E., *Biophys. J.*, *57*, 1075–1084.

[32] Lundbæk, J. A., Maer, A. M., Andersen, O. S., *Biochemistry-Us* 1997, *36*, 5695–5701.

[33] Hassan-Zadeh, E., Hussain, F., Huang, J., *Langmuir* 2017, *33*, 3324–3332.

[34] Beaven, A. H., Maer, A. M., Sodt, A. J., Rui, H., Pastor, R. W., Andersen, O. S., Im, W., *Biophys. J.* 2017, *112*, 1185–1197.

[35] Lalchev, Z. I., Mackie, A. R., *Coll. Surf. B: Biointerfac.* 1999, *15*, 147–160.

[36] Vaz, W. L. C., Clegg, R. M., Hallmann, D., *Biochemistry* 1985, *24*, 781–786.

[37] Antoinette Killian, *J. Biochim. Biophys. Acta (BBA) - Biomem.* 1992, *1113*, 391–425.

[38] Rice, D., Oldfield, E., *Biochemistry* 1979, *18*, 3272–3279.

[39] Lundbaek, J. A., Andersen, O. S., *J.Gen. Physiol.* 1994, *104*, 645–673.

[40] Borisenko, V., Lougheed, T., Hesse, J., Fureder-Kitzmuller, E., Fertig, N., Behrends, J. C., Woolley, G. A., Schutz, G. J., *Biophys. J.* 2003, *84*, 612–622.

[41] Sawyer, D. B., Williams, L. P., Whaley, W. L., Koeppe 2nd, R. E., Andersen, O. S., *Biophys. J.* 1990, *58*, 1207–1212.

[42] Marin-Medina, N., Ramirez, D. A., Trier, S., Leidy, C., *Appl. Microbiol. Biot.* 2016, *100*, 10251–10263.

[43] Hamai, C., Yang, T. L., Kataoka, S., Cremer, P. S., Musser, S. M., *Biophys. J.* 2006, *90*, 1241–1248.

[44] Beaven, A. H., Sodt, A. J., Pastor, R. W., Koeppe, R. E., Andersen, O. S., Im, W., *J. Chem. Theory Comput.* 2017, *13*, 5054–5064.

[45] Lundbaek, J. A., Birn, P., Hansen, A. J., Søgaard, R., Nielsen, C., Girshman, J., Bruno, M. J., Tape, S. E., Egebjerg, J., Greathouse, D. V., Mattice, G. L., Koeppe, R. E. II, Andersen, O. S., *J. Gen. Physiol.* 2004, *123*, 599–621.

[46] Lundbaek, J. A., *J. Gen. Physiol.* 2008, *131*, 421–429.

